JCI insight

Intracellular cholesterol biosynthesis in enchondroma and chondrosarcoma

Hongyuan Zhang, … , Jay S. Wunder, Benjamin A. Alman

JCI Insight. 2019. https://doi.org/10.1172/jci.insight.127232.

Research In-Press Preview Bone biology Oncology

Enchondroma and chondrosarcoma are the most common benign and malignant cartilaginous neoplasms. Mutations in isocitrate dehydrogenase 1 and 2 (*IDH1/2*) are present in the majority of these tumors. We performed RNA-seq analysis on chondrocytes from *Col2a1*Cre;*Idh1*$^{LSL/+}$ animals and found that genes implied in cholesterol synthesis pathway were significantly upregulated in the mutant chondrocytes. We examined the phenotypic effect of inhibiting intracellular cholesterol biosynthesis on enchondroma formation by conditionally deleting SCAP (sterol regulatory element-binding protein cleavage-activating protein), a protein activating intracellular cholesterol synthesis, in IDH1 mutant mice. We found fewer enchondromas in animals lacking SCAP. Furthermore, in chondrosarcomas, pharmacological inhibition of intracellular cholesterol synthesis significantly reduced chondrosarcoma cell viability in vitro and suppressed tumor growth in vivo. Taken together, these data suggest that intracellular cholesterol synthesis is a potential therapeutic target for enchondromas and chondrosarcomas.

Intracellular cholesterol biosynthesis in enchondroma and chondrosarcoma

Hongyuan Zhang[1,2,*], Qingxia Wei[3,4*], Hidetoshi Tsushima[5], Vijitha Puviindran[2], Yuning J. Tang[1,2], Sinthu Pathmanapan[3], Raymond Poon[3], Eyal Ramu[3], Mushriq Al-Jazrawe[3], Jay Wunder[6], Benjamin A. Alman[1,2,4]

1. Department of Cell Biology, Duke University, Durham, NC, USA
2. Department of Orthopeadic Surgery, Duke University, Durham, NC, USA
3. Developmental and Stem Cell Biology, Hospital for Sick Children, Toronto, ON, Canada.
4. First Affiliated Hospital of Xi'an Jiaotong University, Xi'an, Shaanxi, PR China 710061
5. Department of Orthopaedic Surgery, Kyushu Medical Center, Fukuoka, Japan
6. Lunenfeld-Tanenbaum Research Institute, Mount Sinai Hospital, Toronto, ON, Canada.

* These authors contributed equally.

The authors have declared that no conflict of interest exists.

Correspondence:
Dr. Benjamin A. Alman
Duke Hospital South, 200 Trent Drive, Orange Zone 5th floor
DUMC 2888, Durham, NC 27710
919-613-6935
ben.alman@duke.edu

Abstract:

Enchondroma and chondrosarcoma are the most common benign and malignant cartilaginous neoplasms. Mutations in isocitrate dehydrogenase 1 and 2 (*IDH1/2*) are present in the majority of these tumors. We performed RNA-seq analysis on chondrocytes from *Col2a1*Cre;*Idh1*$^{LSL+}$ animals and found that genes implied in cholesterol synthesis pathway were significantly upregulated in the mutant chondrocytes. We examined the phenotypic effect of inhibiting intracellular cholesterol biosynthesis on enchondroma formation by conditionally deleting SCAP (sterol regulatory element-binding protein cleavage-activating protein), a protein activating intracellular cholesterol synthesis, in IDH1 mutant mice. We found fewer enchondromas in animals lacking SCAP. Furthermore, in chondrosarcomas, pharmacological inhibition of intracellular cholesterol synthesis significantly reduced chondrosarcoma cell viability in vitro and suppressed tumor growth in vivo. Taken together, these data suggest that intracellular cholesterol synthesis is a potential therapeutic target for enchondromas and chondrosarcomas.

Introduction:

Cartilage tumors as a group are the most common neoplasms affecting the bone [1]. They include benign tumors such as enchondromas or osteochondromas and malignant chondrosarcomas [2]. Enchondromas arise from dysregulated growth plate chondrocytes that fail to undergo terminal differentiation and remain at the end of the bone [2, 3]. They can occur within the medullary bone as a single lesion or as multiple lesions (enchondromatosis) in conditions termed Ollier disease and Maffucci syndrome [2]. Multiple enchondromas in Maffucci syndrome are associated with up to 50% chance of these lesions undergoing malignant transformation to form chondrosarcomas [3, 4]. Chondrosarcoma is the second most common malignant primary bone tumor and is resistant to chemotherapy and radiation therapy [5]. Somatic mutations in the isocitrate dehydrogenase 1 and 2 *(IDH1* and *IDH2)* genes are identified in the majority of enchondromas, and about half of chondrosarcomas [6-8]. Expression of a mutant *Idh1* in chondrocytes is sufficient to initiate enchondroma formation in mice by disrupting chondrocyte differentiation [9]. When the mutant *Idh1* was expressed in chondrocytes during development, the mice displayed severe defects in chondrocytes differentiation and could not survive after birth. When the mutant *Idh1* was expressed in chondrocytes postnatally, the mice developed enchondromatosis [9]. D-2-hydroxyglutarate (D-2HG), a commonly believed "oncometabolite", is produced from mutant IDH at high levels. However, inhibition of D-2HG production did not alter cell viability of chondrosarcomas, suggesting mutant IDH may promote tumor growth via other mechanisms [4].

Intracellular cholesterol biosynthesis plays a crucial role in chondrocyte development. This process is regulated by the protein SCAP (sterol regulatory element-binding protein cleavage-activating protein). When intracellular cholesterol level is low, SCAP cleaves and activates the

transcription factors SREBPs (sterol regulatory element-binding proteins) [10]. After cleavage, SREBPs are further processed and translocate to the nucleus to activate genes responsible for cholesterol biosynthesis [10]. Genetic deletion of *Scap* in chondrocytes affected their differentiation and viability [11]. In addition, pharmacological inhibition of cholesterol synthesis by statin drugs caused reduced endochondral bone growth and decreased height of the growth plate [12]. Furthermore, statin drugs rescued chondrocyte differentiation and bone length in models of achondroplasia [13].

Deregulation of cholesterol homeostasis has been identified in multiple cancer types and is believed to be an important contributing factor to cancer progression [14]. Upregulation of cholesterol synthesis pathway is associated with decreased patient survival in sarcoma, acute myeloid leukemia, and melanoma [14]. Serum and intracellular cholesterol levels may not always be directly related, and studies suggest that intracellular cholesterol homeostasis may have a more important role in cancers than the serum cholesterol [14]. Despite this information, the role of cholesterol in cartilage tumors is not known.

In this study, we investigated genes that were differentially expressed in *Idh1* mutant chondrocytes and found that genes that are activated in cholesterol biosynthesis were upregulated. To determine the role of cholesterol biosynthesis in enchondroma and chondrosarcoma, we genetically and pharmacologically modulated this pathway and found that inhibition of cholesterol synthesis inhibited cartilage tumor formation and growth.

Results:

Genes that activate intracellular cholesterol synthesis are upregulated in *Idh1*-KI chondrocytes.

IDH1-R132Q was identified in a patient's chondrosarcoma tumor [9]. We generated a mouse expressing IDH1- R132Q in chondrocytes by crossing a mouse expressing a conditional *Idh1*- R132Q knock-in allele [15] with a mouse expressing cre recombinase driven by regulatory elements of the type two collagen gene (*Col2a1*-Cre) [16]. As reported previously, these animals displayed severe defects in chondrocyte differentiation during development and were rarely found alive after birth [9]. They exhibited defects in chondrocyte terminal differentiation. Mice in which the conditional allele was activated postnatally in chondrocytes developed multiple enchondroma-like lesions in the metaphysis of bone [9]. To determine how *Idh1* mutation regulates chondrocyte differentiation, we performed RNA-sequencing analysis on primary sternal chondrocytes isolated from *Col2a1*Cre;*Idh1*$^{LSL/+}$(*Idh1*-KI) animals and *Idh1*$^{LSL/+}$, *Col2a1*Cre littermate controls.

RNA sequencing revealed distinct expression profiles between *Idh1*-KI animals versus the two control groups (GSE123130) (Figure 1A). Gene set enrichment analysis (GSEA) showed that genes regulating cholesterol biosynthesis pathway were significantly upregulated in *Idh1*-KI chondrocytes (Figure 1B). As an example, *Srebf2,* the gene encoding for the transcription factor that activates cholesterol synthesis, was significantly upregulated (Figure 1C). Enzymes in the mevalonate pathway, which is an essential process for cholesterol synthesis, were consistently upregulated in *Idh1*-KI chondrocytes (Figure 1C). We confirmed the upregulation of genes in the pathway such as *Hmgcr,* the rate limiting enzyme in the mevalonate pathway, by qPCR (Figure 1D). To determine changes in cholesterol levels, we performed filipin staining and found significantly higher levels of filipin staining intensity in *Idh1*-KI chondrocytes compared to

chondrocytes from control animals (Figure 2A and 2B). These data consistently suggest cholesterol biosynthesis is activated in chondrocytes expressing mutant *Idh1*.

Deleting *Scap* postnatally did not alter growth plate phenotype

SCAP (sterol regulatory element-binding protein cleavage-activating protein) activates intracellular cholesterol synthesis pathway by cleaving and activating transcription factors SREBPs (sterol regulatory element-binding proteins) [10]. We examined the role of intracellular cholesterol in chondrocytes by genetically deleting *Scap*. We generated *Col2a1*Cre^{ERT2};*Scap*$^{f/f}$ (*Scap*-CKO) mice where *Scap* was conditionally deleted in *Col2a1* expressing cells upon tamoxifen administration at four weeks. Recombination was confirmed by PCR. The phenotype of the growth plate cartilage in *Scap*-CKO mice was examined at 6 month old. Histological evaluation did not reveal an obvious phenotype in the growth plate cartilage of *Scap*-CKO mice (Supplementary Figure 1A). The presence of early stage chondrocytes in the growth plate was not altered, as shown by immunohistochemistry of SOX9 (Supplementary Figure 1B). Hypertrophic differentiation of growth plate chondrocytes was not affected by *Scap* deletion, as shown by immunohistochemistry of type X collagen (Supplementary Figure 1C). Deletion of *Scap* did not cause abnormal cell proliferation, as shown by immunohistochemistry of Ki67 (Supplementary Figure 1D). Together these data suggest growth plate chondrocytes in adult mice were not affected by *Scap* deletion under physiological condition.

Deleting *Scap* reduced enchondroma-like lesion formation in *Idh1*-KI animals.

To determine if intracellular cholesterol synthesis is important in enchondroma formation, we studied it in mice expressing mutant *Idh1* (*Idh1*-KI). We generated *Col2a1*Cre^{ERT2}; *Scap*$^{f/f}$;*Idh1*$^{LSL/+}$

mice where *Scap* deletion and mutant *Idh1* expression were simultaneously induced by tamoxifen administration in *Col2a1* expressing cells. Enchondroma-like lesions still formed in the absence of *Scap* (Figure 3A). However, quantification showed reduced number and size of enchondroma-like lesions in *Idh1*-KI animals lacking *Scap* (Figure 3B-D). These data show that inhibiting cholesterol synthesis reduced enchondroma-like lesion formation in *Idh1*-KI mice.

Pharmacological inhibition of cholesterol synthesis reduced chondrosarcoma growth in vitro and in vivo

Enchondromas can progress into malignant chondrosarcoma. To examine the role of intracellular cholesterol in chondrosarcoma, we first evaluated cholesterol levels in chondrosarcomas with or without *IDH* mutations. We measured cholesterol levels in cryopreserved primary chondrosarcoma tissues from patients with wild type IDH enzymes or mutant IDH1. Chondrosarcoma tumors with mutant *IDH1* had significantly higher cholesterol levels than the tumors with wildtype *IDH1/2* (Figure 4A). To modulate cholesterol synthesis in chondrosarcoma, we treated primary chondrosarcoma cells derived from five different patients with lovastatin, which inhibits HMG-CoA reductase, the rate limiting enzyme in cholesterol biosynthetic pathway [10]. One of the five patient samples was wildtype for *IDH1/2* and the other four samples had *IDH1* mutation. Treatment of chondrosarcoma cells with lovastatin caused a significant reduction of cell viability in vitro (Figure 4B). We also treated chondrosarcoma explants that were derived from the five patients with lovastatin in vitro. The proliferation rate in chondrosarcoma explants was significantly reduced as shown by immunohistochemistry of Ki67 (Figure 4C, D). Chondrosarcoma thus join other tumor types that cholesterol synthesis inhibition reduced their cell viability [17].

To examine the effects of lovastatin on chondrosarcoma growth in vivo, we generated patient-derived xenografts of chondrosarcomas in NOD-scid-gamma mice as previously described [18]. We examined tumor growth in xenografts established from five different patient tumors. Each patient derived chondrosarcoma was xenografted to ten animals. Five animals were treated with vehicle control and five animals were treated with lovastatin. The treatment started 3 to 4 weeks after injection of tumor cells, a time when the tumor became palpable. For each individual human xenograft, control and lovastatin treatments were started at the same time. In sample #1, *IDH1* and *IDH2* were wildtype. Sample #2, #3, #4, and #5 harbor mutations in *IDH1*. After 4 weeks of treatment, tumor weight was measured. Because there was a high degree of variation among tumor weights from different patients, we normalized the tumor weight of each tumor to the average tumor weight of the control group derived from the same patient. Lovastatin treatment caused an average of 30% reduction of tumor weight (Figure 5A). Proliferation rate of the xenografted chondrosarcoma tumors was examined by BrdU staining. The relative proliferation rate was determined by normalizing the percentage of BrdU positive cells of each tumor to the average percentage of BrdU positive cells of the control group derived from the same patient. Lovastatin reduced proliferation in all five patient derived tumor xenografts (Figure 5B, Supplementary Figure 2A). Apoptosis was examined by immunohistochemistry of cleaved caspase 3. The relative apoptosis rated was determined by normalizing the percentage of cleaved caspase 3 positive cells of each tumor to the average percentage of cleaved caspase 3 positive cells of the control group derived from the same patient. Lovastatin treatment increased apoptosis of chondrosarcoma cells in vivo (Figure 5C). For four of five patient-derived xenografts, the average apoptosis rates were increased by lovastatin treatment. For Sample #1 (IDH1/2-wt), the percentage of cleaved caspase 3 positive cells was not altered by lovastatin treatment (Supplementary Figure

2B), suggesting apoptosis in IDH1/2-wt chondrosarcomas might not be affected by inhibition of intracellular cholesterol biosynthesis in vivo.

Discussion:

IDH1/2 are the most commonly mutated genes in enchondroma and chondrosarcoma. Mutation in *Idh1* in chondrocytes causes defects in their terminal differentiation and results in the formation of enchondroma-like lesions. In this study, we found that *Idh1* mutation in chondrocytes increased intracellular cholesterol biosynthesis, which was important in regulating the number and size of enchondroma-like lesions, the viability of chondrosarcoma cells, and the tumor growth of chondrosarcomas.

At the time of analysis, some enchondroma-like lesions had grown separate from the growth plates and some remained attached to the growth plates in both *Col2a1*Cre^{ERT2};*Idh1*$^{LSL/+}$ and *Col2a1*Cre^{ERT2};Scap$^{fl/fl}$;*Idh1*$^{LSL/+}$ animals. In human patients with enchondromatosis, the tumors are located attached to the growth plates initially and stay in this location after the growth plates close. Because the growth plates never close in mice, the enchondroma-like lesions that formed later during growth would remain attached to the growth plate throughout life.

Intracellular cholesterol regulates chondrocyte differentiation under various conditions. During development, genetic deletion of regulators of cholesterol synthesis disrupted the hypertrophic differentiation of chondrocytes and resulted in shortening limbs by altering hedgehog signaling [11]. In an achondroplasia model with FGFR3 gain-of-function mutation, statins restored chondrocyte differentiation and caused significant bone recovery, suggesting cholesterol could regulate chondrocyte differentiation via crosstalk with FGF signaling [13]. In addition, it was reported abnormal cholesterol levels were associated with the development of osteoarthritis [19].

The mechanisms of which cholesterol biosynthesis regulates tumor growth of enchondroma and chondrosarcoma are not fully elucidated. However, deregulation of cholesterol biosynthesis is known to contribute to cancer growth of other cancer types via multiple mechanisms [14]. In

prostate cancer, upregulation of cholesterol via PI3K/AKT/mTOR signaling promoted cancer aggressiveness and bone metastases [14, 20]. In hepatocellular carcinoma and colon cancer, increased mitochondrial cholesterol content induced resistance to apoptosis [14, 21]. Statins have been used alone or combined with other drugs for multiple types of cancers over the past few decades. They have shown to be especially effective in the treatment of mesenchymal-like cancer cells [14, 22].

Previous studies showed expression of wildtype and mutant *Idh1* is activated by SREBP1 and SREBP2 (encoded by *Srebf1* and *Srebf2*) in livers as well as multiple cancer cell lines [23-25], and our study demonstrated mutant *Idh1* upregulated *Srebf2*. Since expression of mutant IDH1 has been previously shown to affect histone modification and DNA methylation [26, 27], it may be possible that expression of *Srebf2* in *Idh1* mutant chondrocytes could be altered via epigenetic changes. Mutant IDH1 is also known to cause metabolic reprogramming, such as changing redox states [28], which could also be a potential mechanism that regulates intracellular cholesterol biosynthesis.

In conclusion, our study demonstrated intracellular cholesterol synthesis was upregulated in *Idh1*-KI chondrocytes. Genetic and pharmacological inhibition of intracellular cholesterol synthesis suppressed growth in enchondroma-like lesions and chondrosarcoma. Our study identified cholesterol synthesis pathway as a potential therapeutic target in enchondroma and chondrosarcoma, which currently do not have any universally effective therapeutics. As *IDH1/2* are also frequently mutated in other cancers such as glioblastoma and acute myeloid leukemia, our data suggested statin drugs could be a potential therapeutic for these cancers as well.

Methods:

Statistics:

For RNA sequencing analysis, the false discovery rate was calculated to control for multiple hypothesis testing. Other statistical analyses were performed using unpaired, two tailed student t-test. Statistical significance was determined as $p<0.05$. All data were presented as mean ± 95% confidence intervals.

Study Approval:

Animal protocols were approved by the Institutional Animal Care and Use Committee at Duke University.

Animals:

Mice used in this study include *Scap*$^{fl/fl}$ mice [29], *Idh1*$^{LSL/+}$ mice [15], *Col2a1*Cre mice [16], *Col2a1*Cre^{ERT2} mice [30], and NOD *scid* gamma (NSG) mice [31]. All the mice other than NSG were on BL6 background. *Idh1*$^{LSL/+}$ mice bear an R132Q mutation rather than an R132H as previously clarified [9]. Adult growth plate and enchondroma-like phenotypes were analyzed on 6-month-old mice. Tamoxifen was administered daily via intraperitoneal injection for 10 days at 100 mg / kg body weight / day at 4 weeks of age. Hind limbs were harvested for histological analysis.

Xenograft:

Primary chondrosarcoma cells derived from five different patients were used in the study. Chondrosarcoma cells derived from each patient were xenografted onto 10 animals, 5 animals for lovastatin treatment and 5 animals for vehicle treatment. One million chondrosarcoma cells were subcutaneously injected to each NSG mouse. Lovastatin and vehicle control treatment started 3 to 4 weeks following injection, a time when the tumor became palpable. For each individual human xenograft, the controls and treatments were started at the same time following implantation. The

mice were treated with lovastatin (4.5 mg/kg/day) or vehicle (100% ethanol) for four weeks. 5 mg/kg bodyweight of BrdU was administered via intravenous infusion 4 hours before sacrificing the mice. Tumors were harvested, weighted, and processed for immunohistochemistry.

Histological Analysis:

Tissue processing: Hind limbs were fixed in 10% neutral buffered formalin for 3 days, decalcified with 14% EDTA for 2 weeks at room temperate, and embedded in paraffin. Xenografted tumors were fixed in 4% PFA overnight. Tissues were sectioned at 5μm and used for Safranin O staining and immunohistochemistry. For type X collagen, antigen retrieval was performed by citrate buffer incubation (85°C, 15min) and hyaluronidase digestions (10mg/ml, 37°C, 30min). For BrdU, Ki67 and cleaved caspase-3, antigen retrieval was performed by boiling the slides in pressure cooker for 3 min in 10 mM citrate buffer (pH=6.0). Endogenous peroxidase was blocked by 3% H_2O_2 /Methanol (v/v) (10min, R.T.) and DAKO kit (30min, R.T.), (Agilent Technologies, Santa clara, CA). The specimen was blocked with 2% horse serum (30min, R.T.) and incubated with antibodies for Col X (1:500, Thermo Fisher X53), Ki67 (DAKO, MIB-1),BrdU (1:50, CST Bu20a), cleaved caspase-3 (1:200, Cell Signaling Asp175) 4°C, overnight.

Quantification of enchondroma like lesions:

Enchondroma-like lesions were firstly detected by Safranin O staining. We stained 1 slide (2 sections, 10 μm) in every 10 slides (100μm) to identify enchondroma-like lesions. We then examined every section of each bone under the microscope to determine the exact number of sections each enchondroma-like lesion spans and identify any lesions that were missed by Safranin O staining. In this way, we examined these lesions continuously. Each section is 5μm thick. The width of each lesion was determined by the number of sections the lesion spanned. For every Safranin O stained section, we manually outlined each lesion and measured lesion area using the

image processing software Fiji Image J. We estimated tumor volume of each animal by adding up the lesion areas of every Safranin O stained section. Relative tumor volume was determined by normalizing the tumor volume of each animal to the average tumor volume of *Col2a1*Cre^{ERT2};*Idh1*$^{LSL/+}$ animals.

Isolation of primary sternal chondrocytes:

Costal chondrocytes were isolated from E18.5 embryos and P4 pups. Mouse sterna and ribs were digested by Pronase (Roche) (2 mg/ml) for 30min with constant agitation at 37°C, washed by PBS, then digested by Collagenase IV (Worthington) (3 mg/ml) for 1 hr in 37°C humidified chamber, washed by PBS, digested by Collagenase IV (0.5 mg/ml) for 16 hr in 37°C humidified chamber, and filtered using 45μm cell strainer.

Culture of primary sternal chondrocytes:

Costal chondrocytes from *Idh1*$^{LSL/+}$ mice were cultured in DMEM with 10% FBS and 1% Penicillin / Streptomycin.

Filipin staining and quantification:

Filipin staining (Abcam ab133116) was performed on sternal chondrocytes according to manufacturer's instructions. Primary sternal chondrocytes were isolated from E18.5 mouse embryos from the same litter. We quantified the fluorescent intensity of the filipin staining using the image processing software Fiji Image J. Outlines of cells were drawn manually. Mean fluorescence intensities of chondrocytes isolated from control and *Col2a1*Cre;*Idh1*$^{LSL/+}$ animals were measured. 10 fields of each sample were used for measurement, and the average of the 10 measurements was used as the intensity of that sample. The relative intensity was given as a ratio of the intensity of each animal normalized to the average intensity of control animals.

RNA-sequencing:

RNA-seq analysis was performed on sternal chondrocytes from *Col2a1*Cre, *Idh1*$^{LSL/+}$, *Col2a1*Cre;*Idh1*$^{LSL/+}$ animals at E18.5. RNA was extracted using RNeasy Mini Kit (QIAGEN). Extracted total RNA quality and concentration was assessed on a 2100 Bioanalyzer (Agilent Technologies) and Qubit 2.0 (ThermoFisher Scientific), respectively. Only extracts with RNA Integrity Number (RIN) greater than 7 were processed for sequencing. RNA-seq libraries were prepared using the commercially available KAPA Stranded mRNA-Seq Kit. In brief, mRNA transcripts were first captured using magnetic oligo-dT beads, fragmented using heat and magnesium, and reverse transcribed using random priming. During the 2nd strand synthesis, the cDNA:RNA hybrid was converted into to double-stranded cDNA (dscDNA) and dUTP incorporated into the 2nd cDNA strand, effectively marking the second strand. Illumina sequencing adapters were then ligated to the dscDNA fragments and amplified to produce the final RNA-seq library. The strand marked with dUTP was not amplified, allowing strand-specificity sequencing. Libraries were indexed using a six base pairs index allowing for multiple libraries to be pooled and sequenced on the same sequencing lane on a HiSeq 4000 Illumina sequencing platform. Before pooling and sequencing, fragment length distribution and library quality was first assessed on a 2100 Bioanalyzer using the High Sensitivity DNA Kit (Agilent Technologies). All libraries were then pooled in equimolar ratio and sequenced. Multiplexing 8 libraries on one lane of an Illumina HiSeq 4000 flow cell yielded about 40 million 50bp single end sequences per sample. Once generated, sequence data was demultiplexed and Fastq files generated using Bcl2Fastq conversion software provided by Illumina.

RNA-sequencing analysis:

RNA-seq data was processed using the TrimGalore toolkit which employs Cutadapt [32] to trim low quality bases and Illumina sequencing adapters from the 3' end of the reads. Only reads that

were 20nt or longer after trimming were kept for further analysis. Reads were mapped to the GRCm38v75 version of the mouse genome and transcriptome [33] using the STAR RNA-seq alignment tool [34]. Reads were kept for subsequent analysis if they mapped to a single genomic location. Gene counts were compiled using the HTSeq tool. Only genes that had at least 10 reads in any given library were used in subsequent analysis. Normalization and differential expression was carried out using the DESeq2 [35] Bioconductor [36] package with the R statistical programming environment. The false discovery rate was calculated to control for multiple hypothesis testing. Gene set enrichment analysis was performed to identify differentially regulated pathways and gene ontology terms for each of the comparisons performed [37].

Chondrosarcoma cell and explant culture:

Chondrosarcoma cells and/or xenograft explants were cultured in MEM-α with 10% FBS and 1% Penicillin / Streptomycin. Cells / explants were treated with 20μM lovastatin and vehicle (100% ethanol) for 48 hours. Cell viability was measured by SRB cell cytotoxicity assay.

Measurement of cholesterol levels:

We measured cholesterol levels from cryopreserved chondrosarcoma tissues using the cholesterol / cholesteryl ester assay kit (Abcam ab65359) according to manufacturer's instruction. 10 mg tissue from each chondrosarcoma was used for the measurement.

Author contributions:

Hongyuan Zhang designed research studies, conducted experiments, analyzed data and wrote the manuscript. Qingxia Wei designed research studies, conducted experiments and analyzed data. Hidetoshi Tsushima, Vijitha Puviindran, Sinthu Pathmanapan and Raymond Poon conducted experiments. Yuning J. Tang, Eyal Ramu, Mushriq Al-Jarawe, and Jay Wunder made intellectual contributions to studies. Benjamin Alman designed research studies.

Acknowledgement:

We acknowledge NIH for the funding R01AR066765.

Reference:

1. Qasem, S.A. and B.R. DeYoung, *Cartilage-forming tumors.* Semin Diagn Pathol, 2014. **31**(1): p. 10-20.
2. Bovée, J.V.M.G., et al., *Cartilage tumours and bone development: molecular pathology and possible therapeutic targets.* Nat Rev Cancer, 2010. **10**(7): p. 481-488.
3. *WHO Classification of Tumours of Soft Tissue and Bone*. 4 ed. WHO Classification of Tumours, , ed. C.D.M. Fletcher, et al. Vol. 5. 2013: IARC.
4. Suijker, J., et al., *Inhibition of mutant IDH1 decreases D-2-HG levels without affecting tumorigenic properties of chondrosarcoma cell lines.* Oncotarget, 2015. **6**(14): p. 12505-19.
5. Leddy, L.R. and R.E. Holmes, *Chondrosarcoma of bone*, in *Orthopaedic Oncology*. 2014, Springer. p. 117-130.
6. Amary, M.F., et al., *Ollier disease and Maffucci syndrome are caused by somatic mosaic mutations of IDH1 and IDH2.* Nature genetics, 2011. **43**(12): p. 1262-1265.
7. Pansuriya, T.C., et al., *Somatic mosaic IDH1 and IDH2 mutations are associated with enchondroma and spindle cell hemangioma in Ollier disease and Maffucci syndrome.* Nat Genet, 2011. **43**(12): p. 1256-61.
8. Amary, M.F., et al., *IDH1 and IDH2 mutations are frequent events in central chondrosarcoma and central and periosteal chondromas but not in other mesenchymal tumours.* J Pathol, 2011. **224**(3): p. 334-43.
9. Hirata, M., et al., *Mutant IDH is sufficient to initiate enchondromatosis in mice.* Proceedings of the National Academy of Sciences, 2015. **112**(9): p. 2829-2834.
10. Mullen, P.J., et al., *The interplay between cell signalling and the mevalonate pathway in cancer.* Nat Rev Cancer, 2016. **16**(11): p. 718-731.
11. Tsushima, H., et al., *Intracellular biosynthesis of lipids and cholesterol by Scap and Insig in mesenchymal cells regulates long bone growth and chondrocyte homeostasis.* Development, 2018.
12. Wu, S. and F. De Luca, *Role of cholesterol in the regulation of growth plate chondrogenesis and longitudinal bone growth.* J Biol Chem, 2004. **279**(6): p. 4642-7.
13. Yamashita, A., et al., *Statin treatment rescues FGFR3 skeletal dysplasia phenotypes.* Nature, 2014. **513**(7519): p. 507.
14. Kuzu, O.F., M.A. Noory, and G.P. Robertson, *The Role of Cholesterol in Cancer.* Cancer Research, 2016. **76**(8): p. 2063.
15. Sasaki, M., et al., *IDH1 (R132H) mutation increases murine haematopoietic progenitors and alters epigenetics.* Nature, 2012. **488**(7413): p. 656-659.
16. Long, F., et al., *Genetic manipulation of hedgehog signaling in the endochondral skeleton reveals a direct role in the regulation of chondrocyte proliferation.* Development, 2001. **128**(24): p. 5099-108.
17. Osmak, M., *Statins and cancer: Current and future prospects.* Cancer Letters, 2012. **324**(1): p. 1-12.
18. Campbell, V.T., et al., *Hedgehog Pathway Inhibition in Chondrosarcoma Using the Smoothened Inhibitor IPI-926 Directly Inhibits Sarcoma Cell Growth.* Molecular Cancer Therapeutics, 2014. **13**(5): p. 1259-1269.

19. Farnaghi, S., et al., *Cholesterol metabolism in pathogenesis of osteoarthritis disease.* Int J Rheum Dis, 2017. **20**(2): p. 131-140.
20. Porstmann, T., et al., *SREBP activity is regulated by mTORC1 and contributes to Akt-dependent cell growth.* Cell metabolism, 2008. **8**(3): p. 224-236.
21. Montero, J., et al., *Mitochondrial cholesterol contributes to chemotherapy resistance in hepatocellular carcinoma.* Cancer Res, 2008. **68**(13): p. 5246-56.
22. Warita, K., et al., *Statin-induced mevalonate pathway inhibition attenuates the growth of mesenchymal-like cancer cells that lack functional E-cadherin mediated cell cohesion.* Sci Rep, 2014. **4**: p. 7593.
23. Shechter, I., et al., *IDH1 gene transcription is sterol regulated and activated by SREBP-1a and SREBP-2 in human hepatoma HepG2 cells: evidence that IDH1 may regulate lipogenesis in hepatic cells.* J Lipid Res, 2003. **44**(11): p. 2169-80.
24. Ricoult, S.J., et al., *Sterol Regulatory Element Binding Protein Regulates the Expression and Metabolic Functions of Wild-Type and Oncogenic IDH1.* Mol Cell Biol, 2016. **36**(18): p. 2384-95.
25. Horton, J.D., et al., *Combined analysis of oligonucleotide microarray data from transgenic and knockout mice identifies direct SREBP target genes.* Proceedings of the National Academy of Sciences, 2003. **100**(21): p. 12027.
26. Turcan, S., et al., *IDH1 mutation is sufficient to establish the glioma hypermethylator phenotype.* Nature, 2012. **483**(7390): p. 479-83.
27. Lu, C., et al., *IDH mutation impairs histone demethylation and results in a block to cell differentiation.* Nature, 2012. **483**(7390): p. 474-8.
28. Cohen, A.L., S.L. Holmen, and H. Colman, *IDH1 and IDH2 Mutations in Gliomas.* Current Neurology and Neuroscience Reports, 2013. **13**(5): p. 345.
29. Matsuda, M., et al., *SREBP cleavage-activating protein (SCAP) is required for increased lipid synthesis in liver induced by cholesterol deprivation and insulin elevation.* Genes Dev, 2001. **15**(10): p. 1206-16.
30. Chen, M., et al., *Generation of a transgenic mouse model with chondrocyte-specific and tamoxifen-inducible expression of Cre recombinase.* Genesis, 2007. **45**(1): p. 44-50.
31. Shultz, L.D., et al., *Human lymphoid and myeloid cell development in NOD/LtSz-scid IL2R gamma null mice engrafted with mobilized human hemopoietic stem cells.* J Immunol, 2005. **174**(10): p. 6477-89.
32. Martin, M., *Cutadapt removes adapter sequences from high-throughput sequencing reads.* EMBnet. journal, 2011. **17**(1): p. pp. 10-12.
33. Kersey, P.J., et al., *Ensembl Genomes: an integrative resource for genome-scale data from non-vertebrate species.* Nucleic acids research, 2011. **40**(D1): p. D91-D97.
34. Dobin, A., et al., *STAR: ultrafast universal RNA-seq aligner.* Bioinformatics, 2013. **29**(1): p. 15-21.
35. Love, M.I., W. Huber, and S. Anders, *Moderated estimation of fold change and dispersion for RNA-seq data with DESeq2.* Genome biology, 2014. **15**(12): p. 550.
36. Huber, W., et al., *Orchestrating high-throughput genomic analysis with Bioconductor.* Nature methods, 2015. **12**(2): p. 115.
37. Mootha, V.K., et al., *PGC-1α-responsive genes involved in oxidative phosphorylation are coordinately downregulated in human diabetes.* Nature genetics, 2003. **34**(3): p. 267.

Figure 1: Cholesterol synthesis pathway is upregulated in *Idh1*-KI chondrocytes.

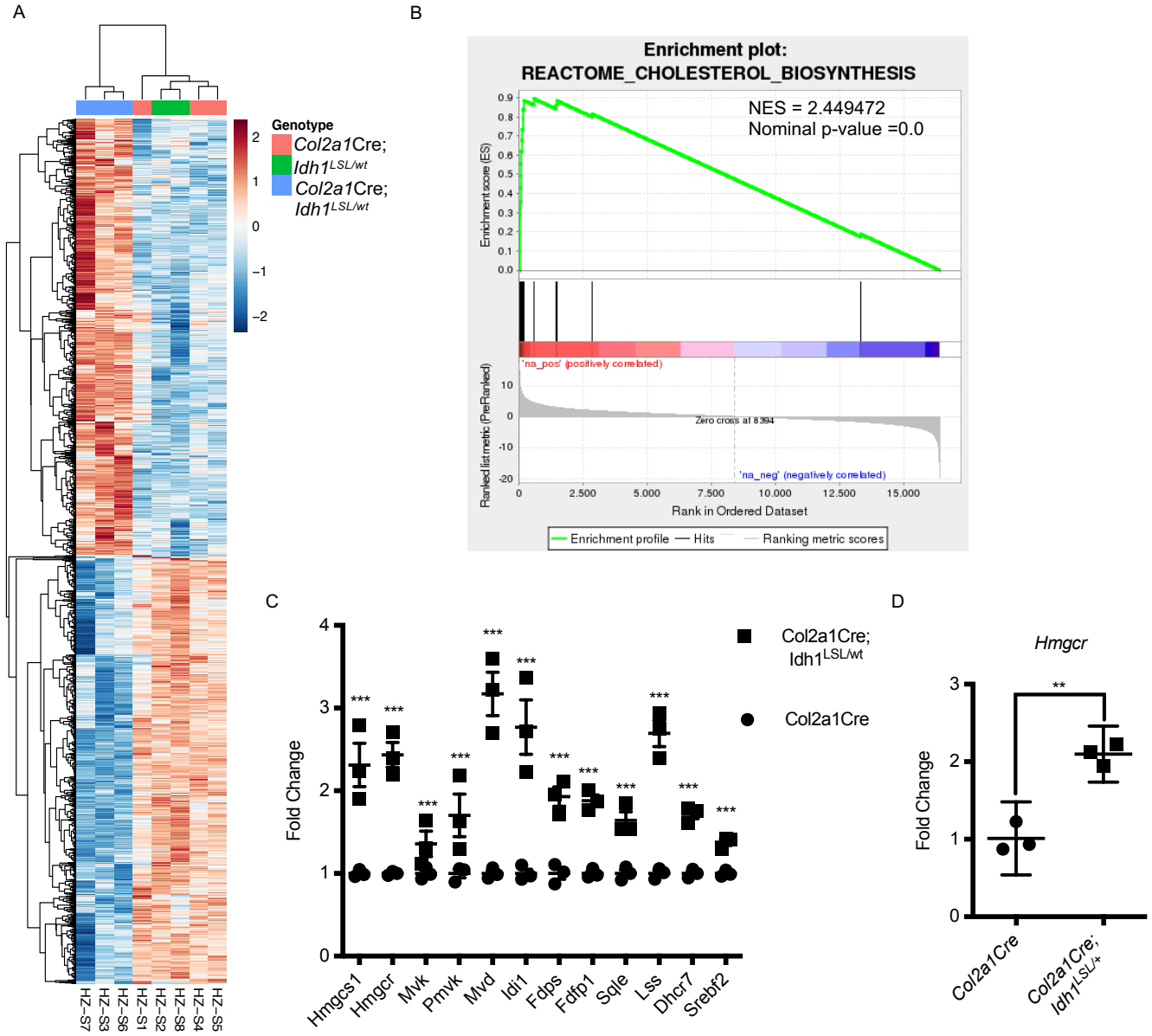

Figure 1: Cholesterol synthesis is upregulated in *Idh1*-KI chondrocytes.
(A) Heatmap of RNA sequencing on sternal chondrocytes from *Col2a1*Cre;*Idh1*$^{LSL/+}$ (n=3), *Idh1*$^{LSL/+}$ (n=2), and *Col2a1*Cre (n=3) mice at E18.5. Littermates were used for the analysis. (B) GSEA analysis for the cholesterol biosynthesis pathway. (C) Relative fold change of gene expression in the cholesterol synthesis pathway (n=3).***p<0.001. The false discovery rate was calculated to control for multiple hypothesis testing. (D) qPCR of *Hmgcr* of sternal chondrocytes isolated from *Col2a1*Cre and *Col2a1*Cre;*Idh1*$^{LSL/+}$ animals at E18.5 (n=3). **p<0.01. p-value was determined by unpaired, two-tailed student t-test. Means ± 95% confidence intervals were shown.

Figure 2: Cholesterol levels were higher in *Idh1*-KI chondrocytes.

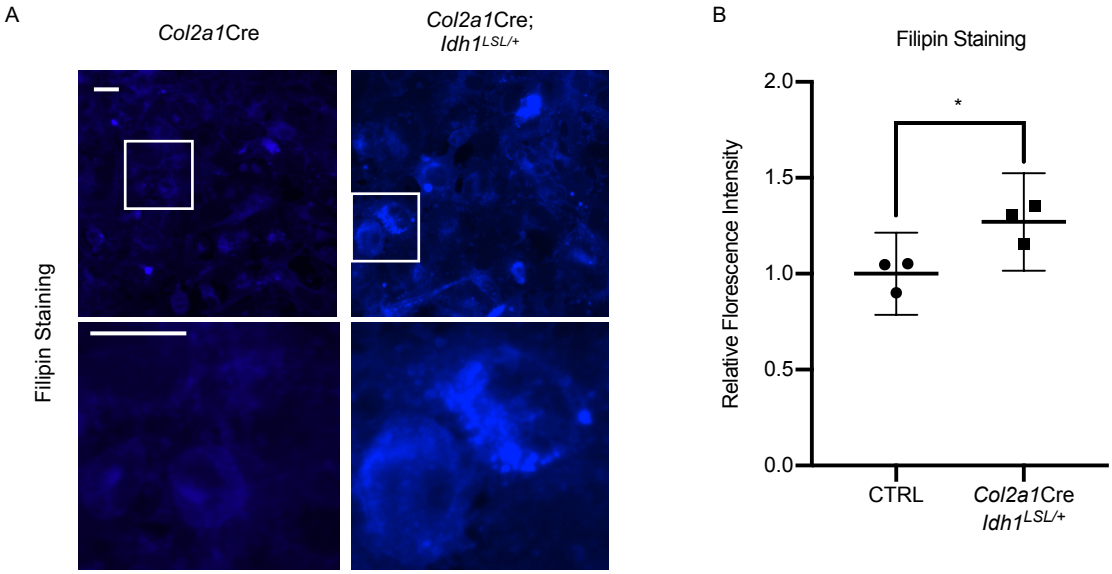

Figure 2: Cholesterol levels were higher in *Idh1*-KI chondrocytes.
(A) Representative filipin staining of sternal chondrocytes isolated from *Col2a1*Cre and *Col2a1*Cre;*Idh1*$^{LSL/+}$ mice at E18.5. (B) Quantification of the filipin staining intensity. The control group included one *Col2a1*Cre animal and two wildtype animals. Littermates were used for the analysis. Scale bars, 25 µm. n=3. *p<0.05. p-value was determined by unpaired, two-tailed student t-test. Means ± 95% confidence intervals were shown.

Figure 3: Deleting *Scap* reduced enchondroma formation in *Idh1-KI* animals.

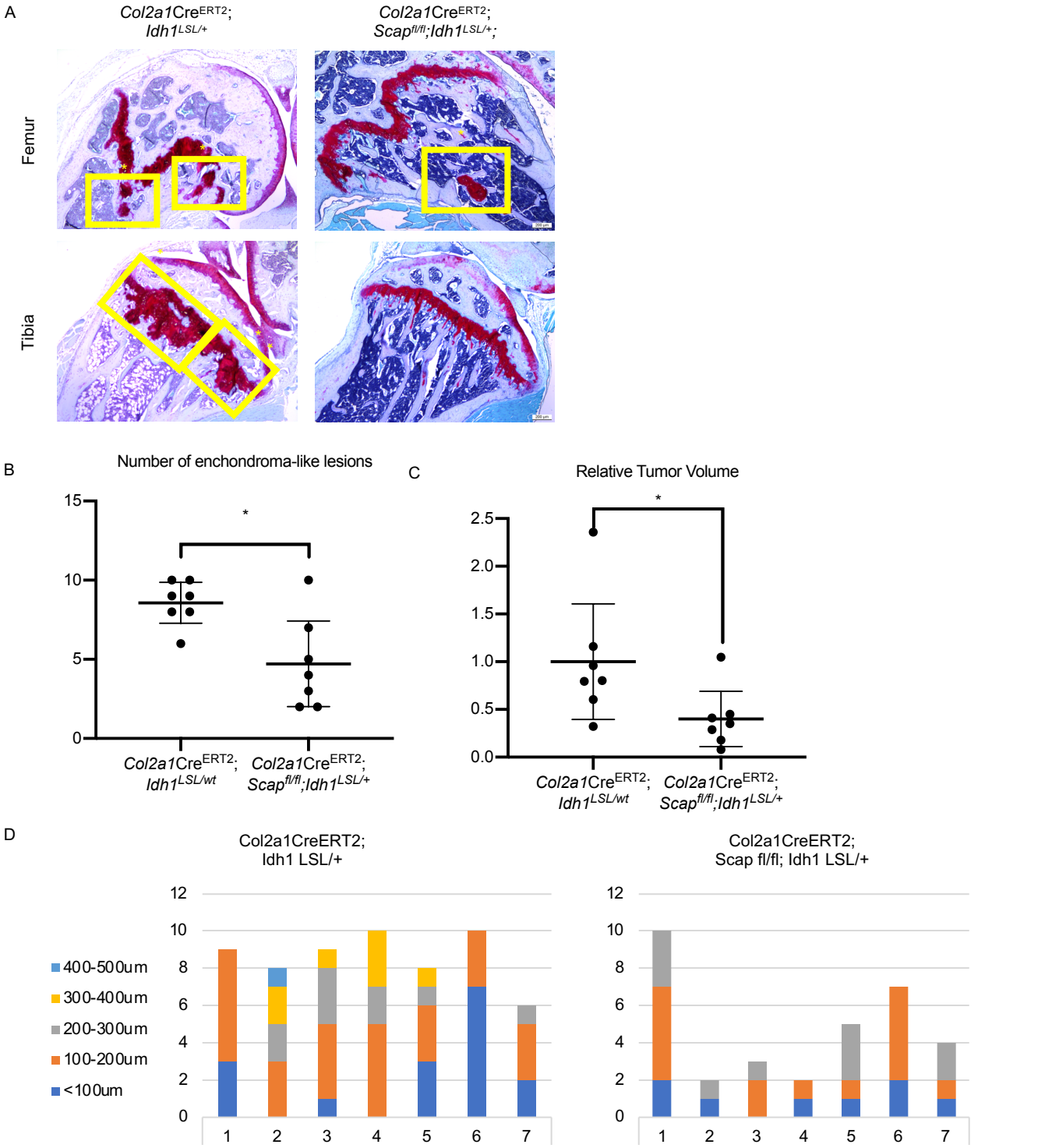

Figure 3: Deleting *Scap* reduced enchondroma-like lesions in *Idh1*-KI mice.
(A) Representative Safranin O staining of *Col2a1*Cre^{ERT2};*Idh1*$^{LSL/+}$ and *Col2a1*Cre^{ERT2};*Scap*$^{fl/f}$;*Idh1*$^{LSL/+}$ mice. (B) Number of enchondroma-like lesions. (C) Relative tumor volume of enchondroma-like lesions. (D) Distribution of the width of enchondroma-like lesions. Scale bars, 200μm. Each data point represents one animal. n=7. *p<0.05. p-value was determined by unpaired, two-tailed student t-test. Means ± 95% confidence intervals were shown.

Figure 4: Lovastatin inhibits chondrosarcoma viability in vitro.

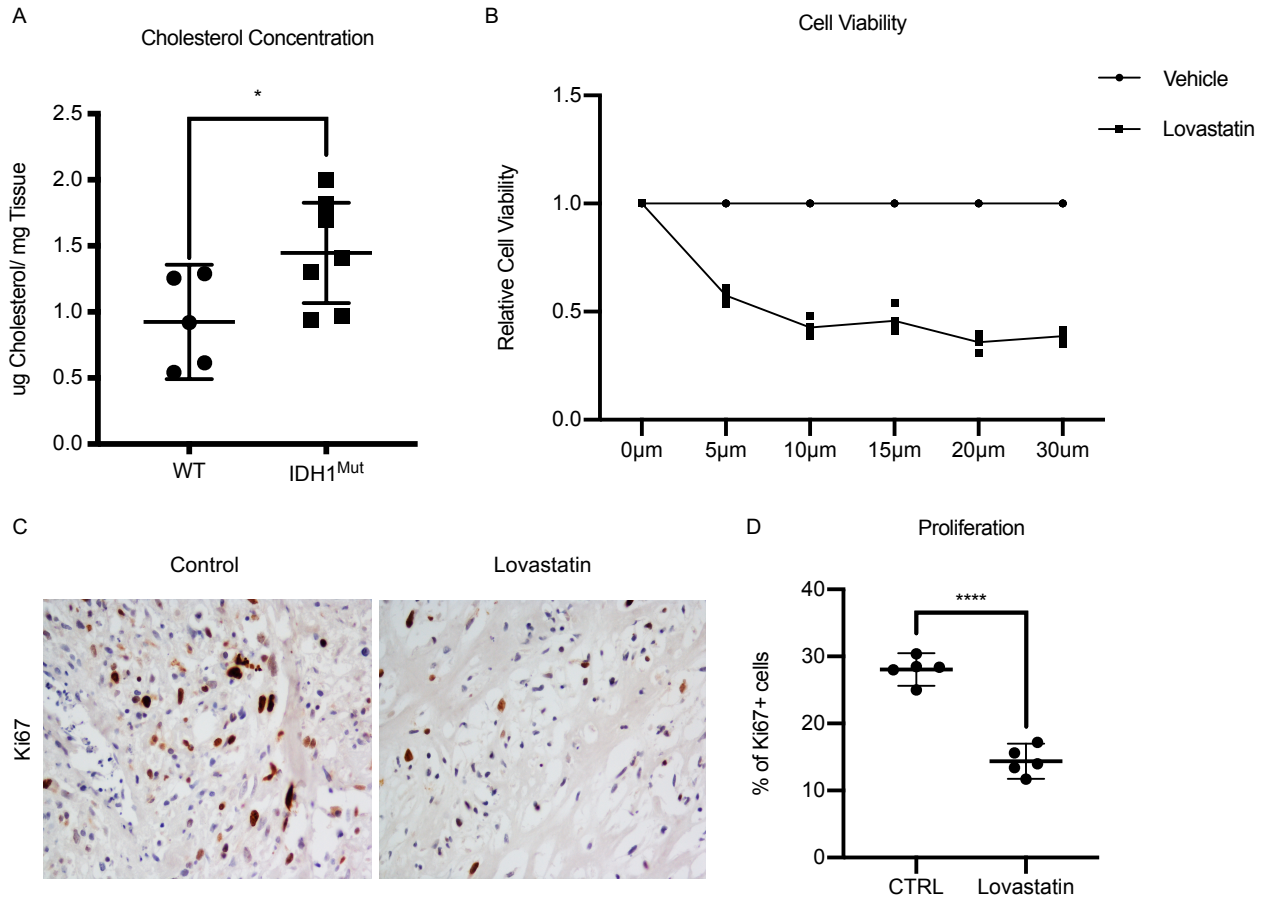

Figure 4: Lovastatin inhibits chondrosarcoma viability in vitro.
(A) Cholesterol concentration in primary chondrosarcoma tumors with wildtype *IDH1/2* (n=5) or mutant *IDH1* (n=7). (B) Relative cell viability of chondrosarcoma cells after lovastatin treatment for 48 hours at indicated concentrations in vitro (n=5). (C) Representative immunohistochemistry for Ki67 on chondrosarcoma explants treated with vehicle control or lovastatin (original magnification, x200). (D) Quantification of the percentage of Ki67 positive cells in (C) (n=5). For Figure 4(A) (B) (D), each data point represents a chondrosarcoma from an individual patient. *p<0.05, ****p<0.0001. p-value was determined by unpaired, two-tailed student t-test. Means ± 95% confidence intervals were shown.

Figure 5: Lovastatin inhibits chondrosarcoma growth in vivo.

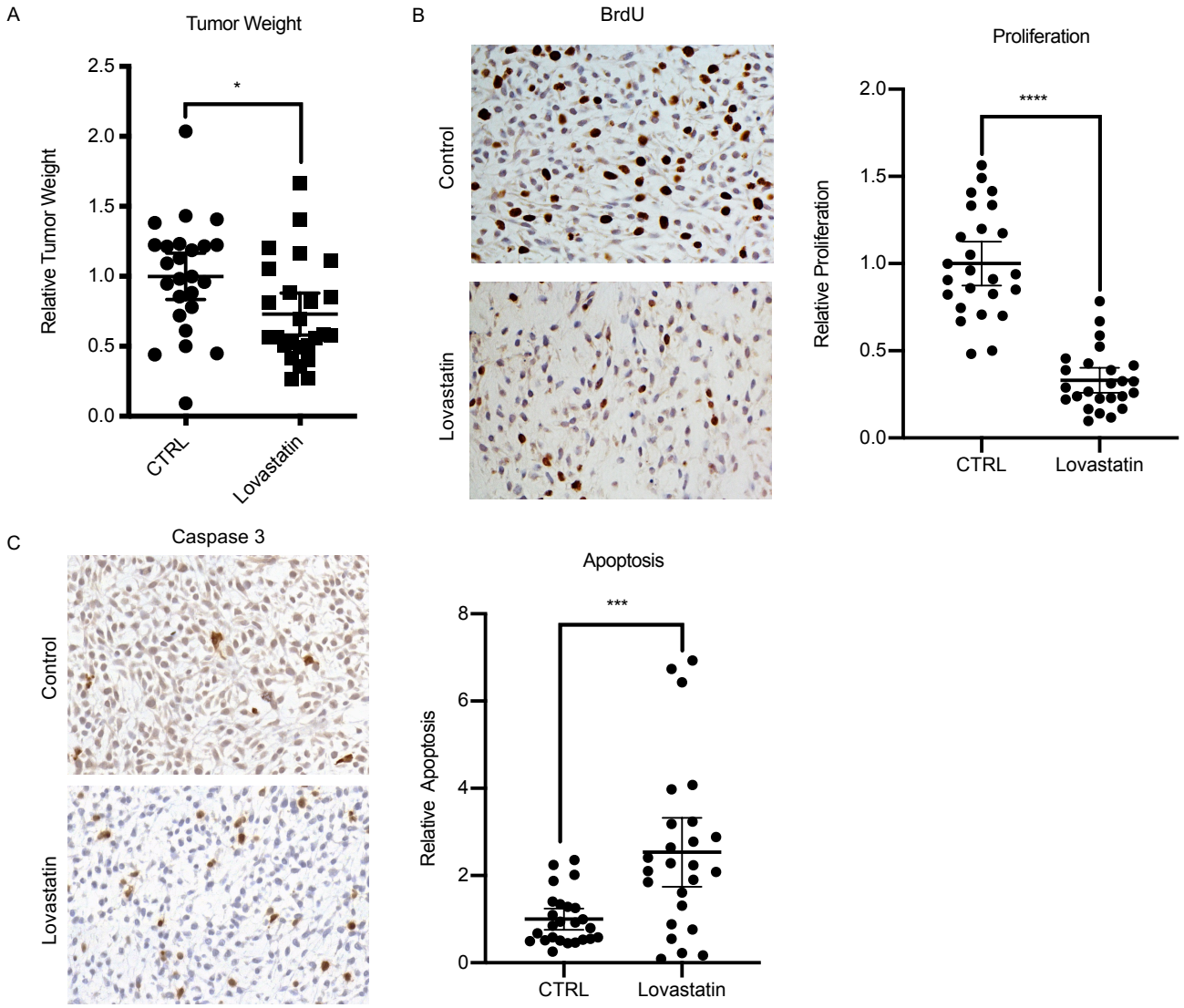

Figure 5: Lovastatin inhibits chondrosarcoma growth in vivo.
(A) Relative tumor weight of chondrosarcoma xenografts after vehicle or lovastatin treatment. (B) Representative figure for BrdU staining on xenografted tumors and quantification of BrdU positive cells in relative values (original magnification, x200). (C) Immunohistochemistry of cleaved caspase 3 on xenografted tumors and quantification of cleaved caspase 3 positive cells in relative values (original magnification, x200). Each data point represents the relative tumor weight, relative percentage of BrdU positive cells, or relative percentage of cleaved caspase 3 positive cells of each xenograft tumor. n=25. *p<0.05, ***p<0.001, ***p<0.0001. p-value was determined by unpaired, two-tailed student t-test. Means $\pm$ 95% confidence intervals were shown.